University of Nebraska - Lincoln

DigitalCommons@University of Nebraska - Lincoln

Xiao Cheng Zeng Publications

Published Research - Department of Chemistry

2016

Unraveling the hidden function of a stabilizer in a precursor in improving hybrid perovskite film morphology for high efficiency solar cells

Zhengguo Xiao
University of Nebraska-Lincoln, zg.xiao1@gmail.com

Dong Wang
University of Nebraska-Lincoln, dwang3@unl.edu

Qingfeng Dong
University of Nebraska-Lincoln, qingfeng.dong@gmail.com

Qi Wang
University of Nebraska-Lincoln

Wei Wei
University of Nebraska-Lincoln

See next page for additional authors

Follow this and additional works at: http://digitalcommons.unl.edu/chemzeng

Part of the Analytical Chemistry Commons, Materials Chemistry Commons, and the Physical Chemistry Commons

Authors

Zhengguo Xiao, Dong Wang, Qingfeng Dong, Qi Wang, Wei Wei, Jun Dai, Xiwei Zheng, and Jinsong Huang

Unraveling the hidden function of a stabilizer in a precursor in improving hybrid perovskite film morphology for high efficiency solar cells†

Zhengguo Xiao,‡[a] Dong Wang,‡[a] Qingfeng Dong,*[a] Qi Wang,[a] Wei Wei,[a] Jun Dai,[b] Xiaocheng Zeng[b] and Jinsong Huang*[a]

The morphology of the organometal trihalide perovskite (OTP) plays a critical role in the performance of solar cell devices. Nevertheless it has been frequently reported that the morphology of OTP films tends to be different in different laboratories even with the same film preparation procedure, which makes it very difficult to compare and understand the material and device physics. Here, we unravel a critical role of the H_3PO_2 stabilizer in HI, which has been largely ignored, in controlling the morphology of the perovskite films. The H_3PO_2 stabilizer in HI solution introduces MAH_2PO_2 impurities into the synthesized MAI (non-purified MAI) by reacting with methylamine (MA) aqueous solution. MAH_2PO_2 impurities can slow down the overall crystallization process of perovskite by forming an intermediate phase of $Pb(H_2PO_2)_2$. Both MAH_2PO_2 and $Pb(H_2PO_2)_2$ impede the fast reaction of PbI_2 and MAI, resulting in highly uniform and smooth perovskite films with larger grain sizes. The recrystallization of non-purified MAI can remove the MAH_2PO_2 impurity and form purified MAI, which however results in rough and non-uniform perovskite films. Uniform and smooth perovskite films can also be obtained by directly adding artificially synthesized MAH_2PO_2 into the purified MAI precursor. This study also suggests $Pb(H_2PO_2)_2$ to be a new precursor to form high quality perovskite films.

Organic–inorganic hybrid perovskite semiconductor materials are emerging as a new generation of solution processed photovoltaic materials which are low cost and nature-abundant.[1–17] A high power conversion efficiency (PCE) of 15–20% has been achieved in both mesoporous structure and planar heterojunction (PHJ) structure devices, with the highest certified efficiency reaching 20.1%.[18] Despite the high efficiency demonstrated, the morphology of the perovskite films, including the grain size

Broader context

The morphologies of the organic–inorganic halide perovskite films play critical roles in affecting the performance of perovskite solar cell devices. However, the issues related to the purity of the perovskite precursors, which critically impact the film morphology, have been largely overlooked in the past. It has been frequently encountered that many high efficiency devices are difficult to reproduce by different or sometimes the same laboratories despite the exactly same reported procedures being strictly followed. Here, we report the discovery that the H_3PO_2 stabilizer in commercial HI solution plays a critical role in controlling the morphology of the perovskite films. H_3PO_2 reacts with CH_3NH_2 (MA) to form MAH_2PO_2 which is blended in the as-synthesized MAI precursor. The reaction of MAH_2PO_2 with PbI_2 forms an intermediate phase of $Pb(H_2PO_2)_2$ which can slow down the crystallization process of $MAPbI_3$ and facilitate the formation of smooth, larger-grain perovskite films. This work highlights the importance of impurities in the precursors.

and crystallinity, is generally found to be different in different laboratories, while it is known that the film morphology is critical in determining the device efficiency and stability.[19] Therefore, it has been frequently encountered that many high efficiency devices are difficult to reproduce even using the same procedures reported. Most of the perovskite morphology optimization is based on the post-treatment of the perovskite films or fabrication methods. However, the issues related to the precursor purity of the perovskite, which are also critical in determining the film morphology, have been largely ignored in the past. In this manuscript, we report the finding that the H_3PO_2 stabilizer in HI solution, which is generally added to prevent the decomposition of HI, plays a critical role in the morphology control of the perovskite films formed, which yields smooth and continuous perovskite thin films for high efficiency devices.

Generally, HI and CH_3NH_2 (MA) aqueous solutions were used as the starting materials for methylammonium iodide (CH_3NH_3I, or MAI) synthesis.[20] The synthesized MAI white powder was washed with diethyl ether (Alfa Aesar) three times to remove the unreacted raw material and/or residual solvent.

[a] *Department of Mechanical and Materials Engineering and Nebraska Center for Materials and Nanoscience, University of Nebraska-Lincoln, Lincoln, NE 68588-0526, USA. E-mail: jhuang2@unl.edu, qingfeng.dong@gmail.com*

[b] *Department of Chemistry, University of Nebraska-Lincoln, Lincoln, NE 68588, USA*

† Electronic supplementary information (ESI) available. See DOI: 10.1039/c6ee00183a
‡ These authors contributed equally.

This journal is © The Royal Society of Chemistry 2016

Energy Environ. Sci., 2016, **9**, 867–872 | **867**

It should be noted that HI solution contains 1.5 wt% H_3PO_2 (Alfa Aesar, L10410) as the stabilizer to prevent HI decomposition. H_3PO_2 can also react with MA to form MAH_2PO_2, which however are hard to be removed by the MAI washing process using diethyl ether. Thus, the as-synthesized MAI still contains MAH_2PO_2 impurities. In order to remove MAH_2PO_2, the as-synthesized MAI could be further purified by a recrystallization process, for example, cooling down the high-temperature supersaturated MAI solution. Due to the high solubility of MAH_2PO_2 in ethanol and its low percentage (1.5 wt%) in MAI, MAH_2PO_2 cannot precipitate during this recrystallization process and thus remains in the solution.[20] Single crystal MAI is obtained after this purification. The obtained purified MAI crystals were washed and dissolved in isopropyl alcohol (IPA) as the precursor. To verify whether MAH_2PO_2 was removed by the recrystallization process, we dissolved both kinds of MAI with equimolar PbI_2 in DMF solution. As shown in Fig. S1 (ESI†), solution (a) using purified MAI was clear and transparent, but solution (b) using non-purified MAI became blur, and white precipitates were observed, which was likely to be the reaction product of MAH_2PO_2 and PbI_2. We also tried to directly synthesis the "purified" MAI (MAI without impurities) using non-stabilized HI solution (Alfa Aesar, 36484). However, the non-stabilized HI is not stable in air and always has yellow/brown color when they are received, which indicates that part of HI decomposed to I_2. Though most of the I_2 could be removed by crystallization using the method described by Lee et al.,[4] the synthesized MAI still showed a light yellow color, which was a strong indication of the presence of residual I_2 impurities.

There are two methods to fabricate the $CH_3NH_3PbI_3$ perovskite films: one-step method using premixed PbI_2 and MAI solution, and a two-step method where PbI_2 and MAI are sequentially deposited.[1,21,22] We have demonstrated that both approaches can produce high efficiency devices with continuous and compact perovskite films.[21,23–25] Here, we mainly focus on the two-step method because it results in a better yield of high efficiency devices. We used both non-purified MAI and purified MAI as precursors for the two-step inter-diffusion method where the PbI_2 and MAI stacking layers were spin-coated sequentially and followed by a thermal annealing process to drive the inter-diffusion of PbI_2 and MAI. In our previous study, the as-synthesized non-purified MAI was used, which yielded uniform and smooth perovskite films.[19,21] The device yield was high with 80% of the devices having an efficiency of over 14.5% using a planar hetero-junction device structure of indium tin oxide (ITO)/poly(3,4-ethylenedioxythiophene):poly(styrenesulphonate) (PEDOT:PSS)/$MAPbI_3$/[6,6]-phenyl-C_{61}-butyric acid methyl ester (PCBM, 10 nm)/C_{60} (20 nm)/2,9-dimethyl-4,7-diphenyl-1,10-phenanthroline (BCP, 8 nm)/aluminum (Al, 100 nm).[21,23] A high stabilized efficiency of 19.4% was reached recently using the as-synthesized MAI by optimizing the hole transporting layers.[26,27] The perovskite films formed on ITO/PEDOT:PSS substrates from the as-synthesized non-purified MAI have mirror like surfaces, and are very uniform in the SEM images shown in Fig. 1a and b. However, when we tried to use purified MAI with an attempt to further increase the perovskite film quality, it was surprising to find that the films
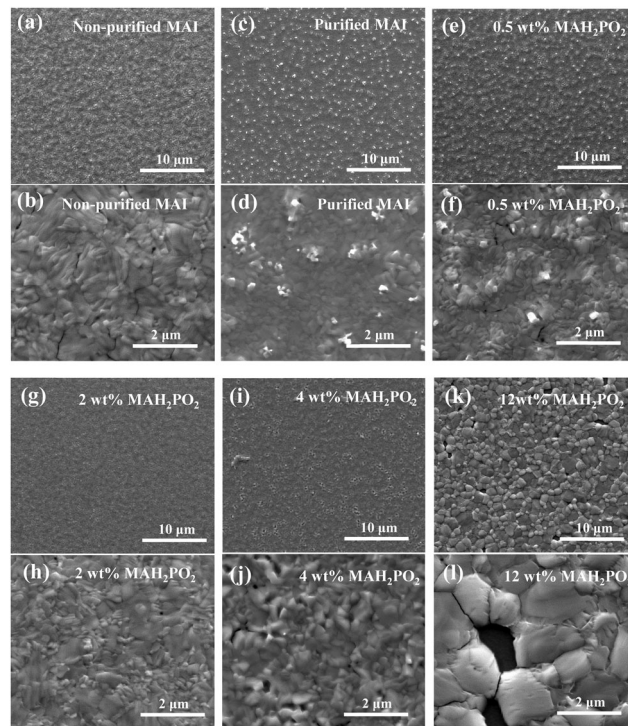

Fig. 1 Top surface images of perovskite films made from (a and b) non-purified MAI, (c and d) purified MAI, (e and f) purified MAI + 0.5 wt% stabilizer, (g and h) purified MAI + 2 wt% stabilizer, (i and j) purified MAI + 4 wt% stabilizer, (k and l) purified MAI + 12 wt% stabilizer.

looked very blur. It is obvious that the perovskite film made from purified MAI is not uniform and has many white spots shown in Fig. 1c and d.

In order to find out the origin of the morphology difference between both types of perovskite films, we examined the effect of possible impurities in the as-synthesized MAI on the film morphology of $MAPbI_3$ perovskite. There are two possible impurities in the as-synthesized MAI powders, which are H_2O and MAH_2PO_2. The non-purified MAI contains approximately 2 wt% MAH_2PO_2 impurities. Besides, MAI is synthesized from the aqueous solution; therefore there might be some H_2O residue in the as-synthesized MAI. Both impurities might affect the nucleation and grain growth processes and the morphology of the perovskite film. We first examined the effect of the possible H_2O residue on the perovskite film morphology. We purposely added different weight ratios of H_2O into the purified MAI solution, then fabricated the perovskite films using the same process as the fabrication of high-performance devices. As shown in Fig. S3 (ESI†), all the perovskite films are not uniform with a surface morphology similar to the perovskite film without adding H_2O. It is reported that the H_2O atmosphere with appropriate humidity (35 ± 5%) can increase the grain growth of perovskite layers, because the moisture can provide an aqueous environment to enhance the transportation of the precursor ions, while high humidity (80%) can cause the decomposition of the perovskite film.[28] Most recently, Leguy et al. reported a similar finding that the hydration of $MAPbI_3$

films goes through a two-step process, first forming a transparent monohydrate of MAPbI$_3$·H$_2$O which is reversible when the films are dehydrated, then converting to dehydrate of MA$_4$PbI$_6$·2H$_2$O which eventually decompose to PbI$_2$. It is irreversible when the perovskite films exposed to liquid water because of the decomposition of MAPbI$_3$.[29,30] But the situation here is different because H$_2$O was evaporated away during the thermal annealing process at 100 °C in a glove box in an open environment. Therefore, the possible contribution of H$_2$O residue in the as-synthesized MAI to the morphology difference can be excluded.

As a next step, we examined the effect of MAH$_2$PO$_2$ impurity in the non-purified MAI on the film morphology. As a control experiment, we synthesized MAH$_2$PO$_2$ by the reaction of H$_3$PO$_2$ with CH$_3$NH$_2$, and purposely blended MAH$_2$PO$_2$ into the purified MAI with different weight ratios from 0 wt% to 12 wt%. We then made perovskite films with these blended MAI:MAH$_2$PO$_2$ as organic precursors, and the top surface SEM images of these perovskite films with different ratios of MAH$_2$PO$_2$ in purified MAI are shown in Fig. 1. With the purified MAI, the film was again very rough. It is interesting that the perovskite films became smoother when an increasing amount of MAH$_2$PO$_2$ from 0 wt% to 2 wt% was added into the purified MAI for the film formation. The grain size also increased with increasing amount of MAH$_2$PO$_2$ (Fig. 1). The film using purified MAI with 2 wt% MAH$_2$PO$_2$ has almost the same morphology with that prepared from as-synthesized non-purified MAI (Fig. 1a and b). It is noticed that the weight ratio of MAH$_2$PO$_2$ in the MAI is 2.1% in the non-purified MAI, because the weight ratio of H$_3$PO$_2$ in the HI solution from Alfa Aesar is 1.5%. The H$_3$PO$_2$ ratio in the HI solution incredibly happens to be the optimized value to yield the best film morphology, explaining the high device efficiency we have achieved using as-synthesized non-purified MAI. When the MAH$_2$PO$_2$ ratio was further increased to 4 wt% and 12 wt% (Fig. 1g), the film became very rough with many pin-holes. Nevertheless, the grain size of the perovskite film

became much larger, which renders us to conclude that MAH$_2$PO$_2$ caused the differences in film morphology.

To figure out how the stabilizer affects the perovskite film morphology, we studied the possible reaction of MAH$_2$PO$_2$ and PbI$_2$ by simulating the same reaction process of MAI and PbI$_2$. As shown in Fig. 2a(I and II), after MAH$_2$PO$_2$ was added into PbI$_2$ solution which was dissolved in DMF, white precipitate formed immediately, which is speculated to result from the following reaction:

$$2MAH_2PO_2 + PbI_2 = Pb(H_2PO_2)_2\downarrow + 2MAI \qquad (1)$$
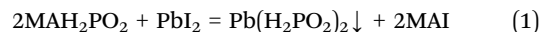
The reaction product, Pb(H$_2$PO$_2$)$_2$, which is insoluble in DMF, was confirmed by analyzing the XRD pattern of the white precipitate (Fig. 2c) which could be well fitted (Fig. 2b and c) with a layered structure. Nevertheless, there was no traceable Pb(H$_2$PO$_2$)$_2$ found in the perovskite films by the XRD study (Fig. S4, ESI†). We therefore speculate that Pb(H$_2$PO$_2$)$_2$ is an intermediate phase for the perovskite formation, which will convert to MAPbI$_3$ in the presence of excess amount of MAI in the perovskite formation process. To verify this speculation, Pb(H$_2$PO$_2$)$_2$ powder was rinsed by DMF to wash off residual PbI$_2$, and re-dispersed in DMF (Fig. 2a(III)), and then a large amount of MAI was added into DMF. As speculated, the white powder slowly dissolved back into DMF solution in the presence of MAI, resulting in a yellow solution (Fig. 2a(IV)), which indicates that reaction (1) is reversible. After drop-casting the yellow solution onto the ITO substrate, we got oil like viscous materials which resemble the as synthesized MAH$_2$PO$_2$, which did not dry in minutes at room temperature. After a high temperature thermal annealing process, it slowly converted into black films (Fig. 2a(V–VII)), which were confirmed to be perovskite by XRD (Fig. 2c), absorption and PL measurements (Fig. S5, ESI†). Since the produced Pb(H$_2$PO$_2$)$_2$ in reaction (1) was able to convert to perovskite again during the thermal
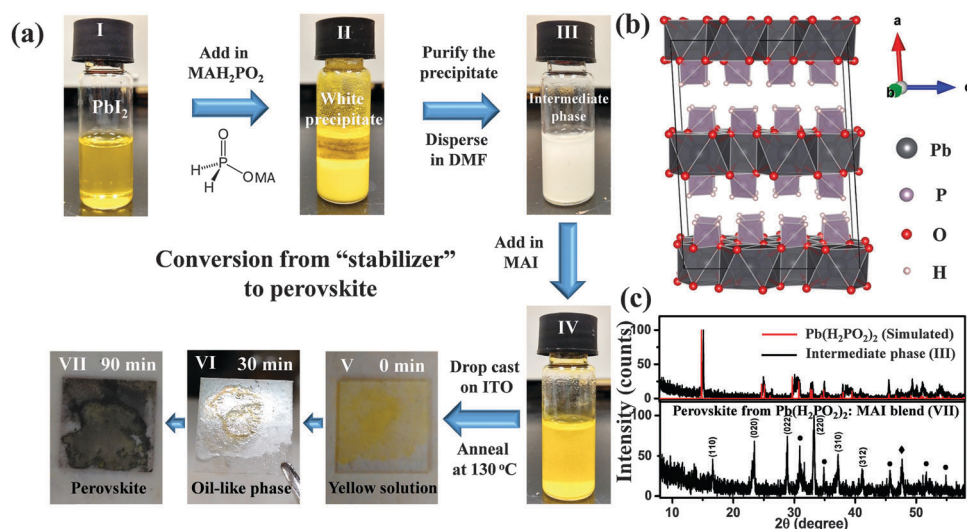

Fig. 2 (a) The conversion from "stabilizer" to perovskite; (b) analyzed crystal structure of the intermediate phase of Pb(H$_2$PO$_2$)$_2$; (c) simulated XRD pattern of Pb(H$_2$PO$_2$)$_2$, the XRD pattern of the intermediate phase and the XRD pattern of the perovskite obtained from Pb(H$_2$PO$_2$)$_2$: MAI blend. "●" is the peak of Pb(H$_2$PO$_2$)$_2$, "◆" is the peak of MAI.

annealing process, we conclude that $Pb(H_2PO_2)_2$ is an intermediate phase during perovskite formation.

It was worth noting that the conversion from $Pb(H_2PO_2)_2$ to perovskite by thermal annealing was much slower than the reaction of PbI_2 and MAI. Reaction (1) is reversible, and therefore the intermediate phase of $Pb(H_2PO_2)_2$ and MAH_2PO_2 coexist. As MAH_2PO_2 is slowly evaporated during the thermal annealing process, the reversible reaction moves to the left, and finally all the intermediate phase converts to perovskite in the presence of excess MAI. Considering that MAH_2PO_2 has a higher boiling point than MAI, both longer and higher temperature is necessary for the conversion of $Pb(H_2PO_2)_2$ to perovskite. It took more than an hour for $Pb(H_2PO_2)_2$ to convert into perovskite even under the high temperature annealing of 130 °C (Fig. 2a(V–VII)). Thus, the presence of MAH_2PO_2 impurities in the MAI precursor could efficiently slow down the reaction of PbI_2 and MAI, yielding a smoother perovskite film. This is very similar to the function of HI that can form an intermediate phase of $HPbI_3$ to slow down the reaction.[31]

Based on the above discussion about the behavior of the intermediate phase in DMF solution, we get a conclusion on the function of the stabilizer during the perovskite crystallization process in the two-step inter-diffusion method (Fig. 3). When purified MAI is used (Fig. 3a), MAI quickly diffuses into the underlying PbI_2 and react with PbI_2 very fast during the thermal-annealing process and form many grains quickly but not continuous films. Once the grains are formed, it is not feasible to spread out or flatten the grains even by long thermal annealing, and the formed perovskite films are not uniform (Fig. S6, ESI†). On the contrary, while using non-purified MAI with MAH_2PO_2 as impurity (Fig. 3b), the $Pb(H_2PO_2)_2$ intermediate phase is formed immediately after MAH_2PO_2 contacts PbI_2, which tends to slow down the reaction of MAI and PbI_2. The $Pb(H_2PO_2)_2$ intermediate phase needs much longer time to convert into perovskite. Meanwhile the oil-like MAH_2PO_2 is formed again during this conversion process, which glues the formed perovskite grains. Thus, the overall formation process of perovskite is slowed down and continuous perovskite films are obtained.

The planar heterojunction structure device with a structure of $ITO/PEDOT:PSS/MAPbI_3/PCBM/C_{60}/BCP/Al$ was fabricated to examine the effect of the stabilizer on the device performance. The photocurrent hysteresis is unique for perovskite solar cells. Therefore, how to correctly measure the performance of perovskite solar cells is critical when there is photocurrent hysteresis. It was suggested that long delay times of at least 5 s after a voltage step before sampling the current should be used in order to get steady state performances when there is hysteresis.[32] Nevertheless, the passivation of the traps at the perovskite film surface and grain boundaries by fullerene was found to eliminate the photocurrent hysteresis of our devices at room temperature.[21,33] Thus, we used photocurrent curves measured at 0.13 V s^{-1} as representative curves for the comparison between the devices with and without MAH_2PO_2 in the MAI precursors. As shown in Fig. 4, both short circuit current and the fill factor increased with the amount of MAH_2PO_2 in the purified MAI increased from 0 wt% to 2 wt%. The device performance of the device with 4 wt% MAH_2PO_2 in the MAI precursor became worse due to the non-uniform films as shown in Fig. 1. The performance of the device with 2 wt% MAH_2PO_2 is comparable with the device made from non-purified MAI. The power conversion efficiencies (PCEs) of the devices are shown in Table 1. The reduced efficiency of the device with purified MAI can be explained by the possible increased recombination rate due to the incomplete passivation of the traps of the rough perovskite surface. It also should be noticed that the photocurrent hysteresis of the devices also decreased with increasing amount of MAH_2PO_2 from 0 wt% to 2 wt% in the purified MAI. This is consistent with our previous reports that charge traps are one of the origins for the photocurrent hysteresis, and the passivation of the traps can reduce the photocurrent hysteresis. Reduced trap density after adding MAH_2PO_2 is confirmed by the dark current. As shown in Fig. 4f, the dark current was increased under large forward bias after adding MAH_2PO_2. This indicated that there were fewer traps in the films, which might be due to the larger grains and/or more uniform films formed with MAH_2PO_2 (Fig. 1). The current minimum did not coincide with 0 V applied bias which might be caused by ion motion and/or the traps in the perovskite layer. It should be noted that a much higher efficiency of 18–20% has been achieved by applying a non-wetting hole transport layer using the precursor with the stabilizer.[26,27] Here we only compared
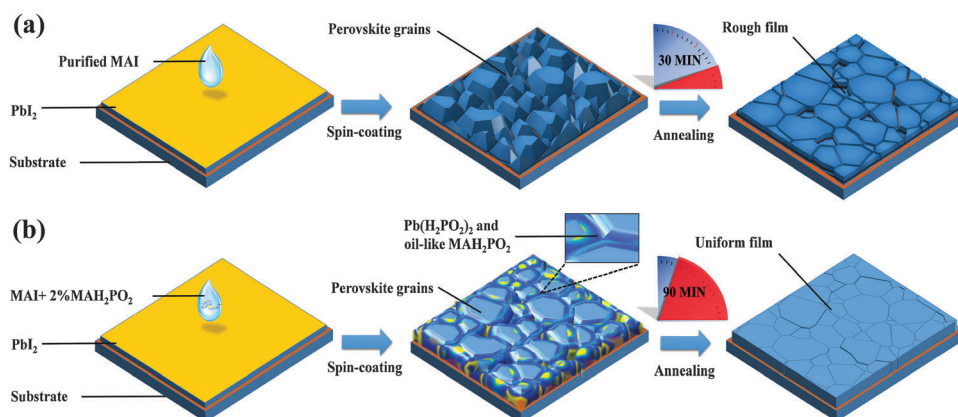

Fig. 3 Schematic diagram of the perovskite crystallization process (a) without and (b) with a stabilizer (MAH_2PO_2) in the precursor.

870 | Energy Environ. Sci., 2016, 9, 867–872

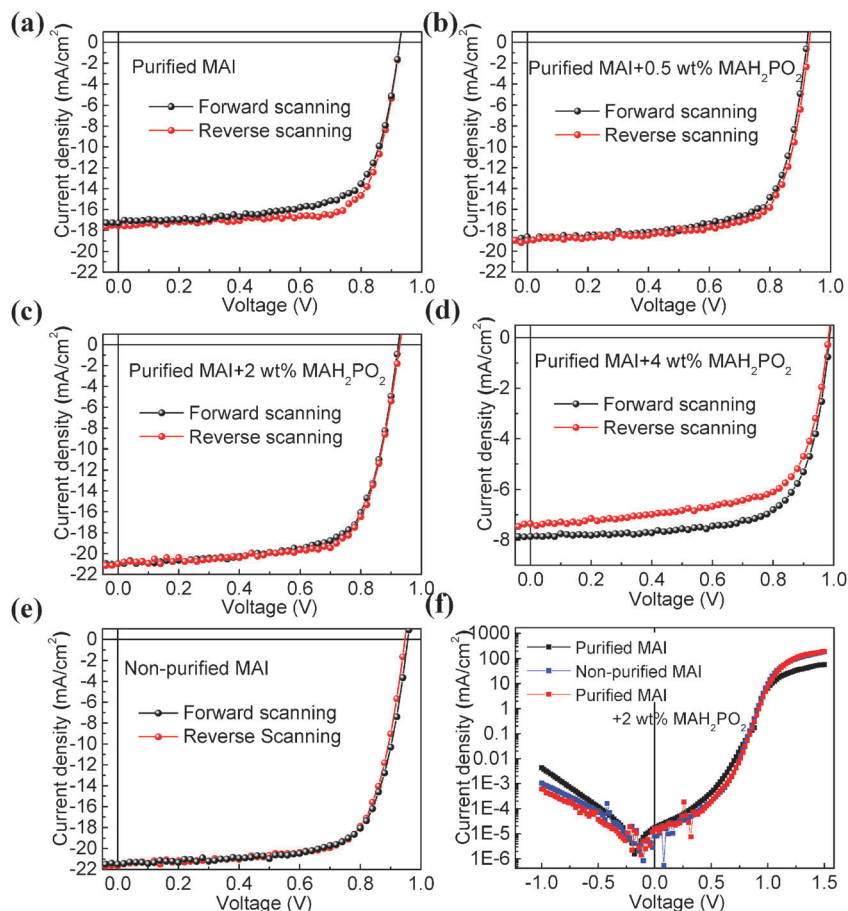This journal is © The Royal Society of Chemistry 2016

Fig. 4 Photocurrent curves of the device with different weight ratios of MAH_2PO_2 in the MAI precursors (a) 0 wt%, (b) 0.5 wt%, (c) 2 wt%, (d) 4 wt%. (e) Photocurrent curves of the device using non-purified MAI as the precursor. (f) Dark current curves of the devices with different kinds of organic precursors.

Table 1 Power conversion efficiency of devices measured in Fig. 4

	Purified MAI	Purified MAI + 0.5 wt% MAH_2PO_2	Purified MAI + 2 wt% MAH_2PO_2	Purified MAI + 4 wt% MAH_2PO_2	Non-purified MAI
Forward scanning	11.1%	12.3%	13.5%	5.4%	14.5%
Reverse scanning	11.9%	12.7%	13.9%	4.9%	14.5%

the device performance on PEDOT:PSS to be consistent with the morphology study.

In conclusion, we unraveled the critical role of the stabilizer in HI solution on the morphology of two-step fabricated perovskite films. The existence of MAH_2PO_2 impurity can significantly slow down the fast reaction between PbI_2 and MAI by forming an intermediate phase $Pb(H_2PO_2)_2$ during spin-coating the non-purified MAI onto PbI_2 film. The reaction of MAH_2PO_2 with PbI_2 is reversible, thus $Pb(H_2PO_2)_2$ can slowly convert to perovskite in the presence of excess MAI during thermal annealing. Based on this finding, we can control the crystallization rate of perovskite by tuning the ratio of MAH_2PO_2 in the MAI precursor in order to improve film morphology. The higher MAH_2PO_2 ratio is in favor of larger grains but may leave pin-holes in the final film. It has been proved that 2 wt% MAH_2PO_2 in MAI can produce the most uniform perovskite film. This content happens to match with the content of H_3PO_2 in HI solution, which explains why the former reported perovskite films had high quality. The discovery of the function of the stabilizer enriches the formation mechanism of perovskite thin films, which is helpful for the improvement of device reproducibility and development of high efficiency perovskite solar cells.

Author contributions

The manuscript was written through contributions of all authors. All authors have given approval to the final version of the manuscript.

Conflicts of interest

The authors declare no competing financial interest.

This journal is © The Royal Society of Chemistry 2016

Energy Environ. Sci., 2016, 9, 867–872 | 871

Acknowledgements

References

1 J. Burschka, N. Pellet, S.-J. Moon, R. Humphry-Baker, P. Gao, M. K. Nazeeruddin and M. Grätzel, *Nature*, 2013, **499**, 316.

2 M. Liu, M. B. Johnston and H. J. Snaith, *Nature*, 2013, **501**, 395.

3 A. Kojima, K. Teshima, Y. Shirai and T. Miyasaka, *J. Am. Chem. Soc.*, 2009, **131**, 6050.

4 M. M. Lee, J. Teuscher, T. Miyasaka, T. N. Murakami and H. J. Snaith, *Science*, 2012, **338**, 643.

5 A. Abrusci, S. D. Stranks, P. Docampo, H.-L. Yip, A. K. Y. Jen and H. J. Snaith, *Nano Lett.*, 2013, **13**, 3124.

6 J. M. Ball, M. M. Lee, A. Hey and H. J. Snaith, *Energy. Environ. Sci.*, 2013, **6**, 1739.

7 G. Hodes, *Science*, 2013, **342**, 317.

8 J. Y. Jeng, Y. F. Chiang, M. H. Lee, S. R. Peng, T. F. Guo, P. Chen and T. C. Wen, *Adv. Mater.*, 2013, **25**, 3727.

9 H.-S. Kim, I. Mora-Sero, V. Gonzalez-Pedro, F. Fabregat-Santiago, E. J. Juarez-Perez, N.-G. Park and J. Bisquert, *Nat. Commun.*, 2013, **4**, 2242.

10 N.-G. Park, *J. Phys. Chem. Lett.*, 2013, **4**, 2423.

11 H. J. Snaith, *J. Phys. Chem. Lett.*, 2013, **4**, 3623.

12 S. D. Stranks, G. E. Eperon, G. Grancini, C. Menelaou, M. J. Alcocer, T. Leijtens, L. M. Herz, A. Petrozza and H. J. Snaith, *Science*, 2013, **342**, 341.

13 W. Zhang, M. Saliba, S. D. Stranks, Y. Sun, X. Shi, U. Wiesner and H. J. Snaith, *Nano Lett.*, 2013, **13**, 4505.

14 G. Xing, N. Mathews, S. Sun, S. S. Lim, Y. M. Lam, M. Grätzel, S. Mhaisalkar and T. C. Sum, *Science*, 2013, **342**, 344.

15 J. H. Heo, S. H. Im, J. H. Noh, T. N. Mandal, C.-S. Lim, J. A. Chang, Y. H. Lee, H.-j. Kim, A. Sarkar and M. K. Nazeeruddin, *Nat. Photonics*, 2013, **7**, 486.

16 N.-G. Park, *J. Phys. Chem. Lett.*, 2013, **4**, 2423.

17 P. Docampo, J. M. Ball, M. Darwich, G. E. Eperon and H. J. Snaith, *Nat. Commun.*, 2013, **4**, 2761.

18 M. A. Green, K. Emery, Y. Hishikawa, W. Warta and E. D. Dunlop, *Prog. Photovoltaics*, 2015, **23**, 1.

19 G. E. Eperon, V. M. Burlakov, P. Docampo, A. Goriely and H. J. Snaith, *Adv. Funct. Mater.*, 2014, **24**, 151.

20 Y. Deng, E. Peng, Y. Shao, Z. Xiao, Q. Dong and J. Huang, *Energy. Environ. Sci.*, 2015, **8**, 1544.

21 Z. Xiao, C. Bi, Y. Shao, Q. Dong, Q. Wang, Y. Yuan, C. Wang, Y. Gao and J. Huang, *Energy Environ. Sci.*, 2014, **7**, 2619.

22 Q. Chen, H. Zhou, Z. Hong, S. Luo, H.-S. Duan, H.-H. Wang, Y. Liu, G. Li and Y. Yang, *J. Am. Chem. Soc.*, 2013, **136**, 622.

23 Z. Xiao, Q. Dong, C. Bi, Y. Shao, Y. Yuan and J. Huang, *Adv. Mater.*, 2014, **26**, 6503.

24 M. Xiao, F. Huang, W. Huang, Y. Dkhissi, Y. Zhu, J. Etheridge, A. Gray-Weale, U. Bach, Y. B. Cheng and L. Spiccia, *Angew. Chem.*, 2014, **126**, 10056.

25 N. J. Jeon, J. H. Noh, Y. C. Kim, W. S. Yang, S. Ryu and S. I. Seok, *Nat. Mater.*, 2014, **13**, 897.

26 C. Bi, Q. Wang, Y. Shao, Y. Yuan, Z. Xiao and J. Huang, *Nat. Commun.*, 2015, **6**, 7747.

27 Y. Shao, Y. Yuan and J. Huang, *Nature Energy*, 2016, **1**, 15001.

28 J. You, Y. M. Yang, Z. Hong, T.-B. Song, L. Meng, Y. Liu, C. Jiang, H. Zhou, W.-H. Chang and G. Li, *Appl. Phys. Lett.*, 2014, **105**, 183902.

29 A. M. Leguy, Y. Hu, M. Campoy-Quiles, M. I. Alonso, O. J. Weber, P. Azarhoosh, M. Van Schilfgaarde, M. T. Weller, T. Bein and J. Nelson, *Chem. Mater.*, 2015, **27**, 3397.

30 S. Wozny, M. Yang, A. M. Nardes, C. C. Mercado, S. Ferrere, M. O. Reese, W. Zhou and K. Zhu, *Chem. Mater.*, 2015, **27**, 4814.

31 F. Wang, H. Yu, H. Xu and N. Zhao, *Adv. Funct. Mater.*, 2015, **25**, 1120.

32 E. Unger, E. Hoke, C. Bailie, W. Nguyen, A. Bowring, T. Heumüller, M. Christoforo and M. McGehee, *Energy Environ. Sci.*, 2014, **7**, 3690.

33 Y. Shao, Z. Xiao, C. Bi, Y. Yuan and J. Huang, *Nat. Commun.*, 2014, **5**, 5784.